Desalination and Water Treatment
www.deswater.com
doi: 10.5004/dwt.2023.29674

298 (2023) 127–135
June

Fixed bed column adsorption of phenol onto locally available soil: linear kinetics modeling

Busetty Subramanyam

School of Civil Engineering, Centre for Advanced Research in Environment (CARE), SASTRA Deemed University, Thanjavur, India 613401, email: subramanyamjy@gmail.com/subramanyam@civil.sastra.edu

Received 17 January 2023; Accepted 7 June 2023

ABSTRACT

In the present study analysis of fixed column adsorption studies of phenol onto the soil was investigated. The soil minerals were characterized by of X-ray diffraction peaks at diffraction angles of 21.208, 26.985 and 50.509 and adsorption studies were conducted at a pH of 6.00. The effects of process variables on the bed performance were studied, these included flow rate and bed depth. The results showed that a decrease in flow rate at a constant bed depth increased the breakthrough volume (V_b) and therefore the breakthrough time (T_b), due to an increase in empty bed contact time (EBCT). At the flow rate of 10 mL/min and at varying depths 5, 10 and 15 cm the EBCT was found 2.45, 4.91 and 7.36 min. Similarly for a flow rate of 20 and 30 mL/min, at varying depths 5, 10 and 15 cm, the EBCT was found 1.23, 2.45 and 3.68 min and 0.82, 1.64 and 2.45 min, respectively. For these test columns, the optimum flow rate should not be higher than 10 mL/min to provide a shorter adsorption zone and a longer service time. The adsorption capacity (N_o) of soil was calculated to be 713.37, 978.34 and 978.34 mg/L by using the flow rates of 10, 20 and 30 mL/min. The results of the examination of the dynamic adsorption system were also demonstrated to be significantly influenced by the modelling methodology.

Keywords: Fixed column; Empty bed contact time (EBCT); Bed depth service time (BDST); Break though curves; Adsorption; Flow rate

1. Introduction

Growing wastewater has been a result of the global industrial production sector's quick development. Water quality is decreased when wastewater is discharged, making it impossible to use water without first desalinating it for drinking purposes and other industrial uses [1–3]. Even at low concentrations, wastewater including resins, dyes, pesticides, phenol, and phenolic compounds may endanger the lives of people as well as aquatic life [4]. The production of pharmaceuticals, personal care products, nylon, resins, pulp and paper mills, coal gasification operating units, and petroleum refineries and industries so on so forth use phenols. Due to its carcinogenic characteristics and extreme difficulty in biological degradation, it is categorised as extremely hazardous [5]. Fish have toxic phenol levels between 9 and 25 mg/L, while human toxic phenol levels are between 10 and 24 mg/L. Around 150 mg/100 mL is the fatal quantity in human blood. But there are numerous methods for recovering and getting rid of phenol. The most popular techniques include steam stripping, ion exchange, adsorption, hot gases, and solvent extraction. These techniques have been discovered to be effective for removing phenol [6–10]. These methods remove phenol directly form water and wastewater. Whereas the biological treatment process also removes phenol, phenolic wastewater is passed through activated carbon in moving, fixed, or fluidized beds.

To evaluate the feasibility and economics of adsorbent, a laboratory study is usually conducted. The batch study gives the removal capacity of specific waste contaminants,

but the continuous flow provides practical application of the process. For industrial application fixed bed adsorption column study is an important step [11,12]. The breakthrough curves must be predictable under predetermined operating circumstances for a packed bed adsorption process to be properly designed and operated [13]. It is required to stop the adsorption period in a process before the saturation, a thorough understanding of adsorption characteristics is necessary [14]. At industrial scale, the effects of design parameters, such as bed height and flow rate, have been investigated. The column study for adsorption starts with laboratory testing to establish the breakthrough curve. The amount of adsorbate adsorbed within a bed depends both on space and time. As fluid enters the bed, it meets the first few layers of absorbent. Solute adsorbs, filling up some of the available sites [15]. As the top layers of adsorbent become saturated with adsorbate, the mass transfer zone (MTZ) will move down in the bed until breakthrough occurs. The length of the MTZ is typically a function of the hydraulic loading rate applied to the column and the characteristics of the adsorbent.

There are many different types of techniques by which the main point of contact between adsorbate and adsorbent occurs in the adsorption system, including batch, continuous moving bed, continuous fixed bed (up flow or downflow), continuous fluidize bed, and pulsed bed. A representation of the pollutant-effluent concentration vs. time profile in a fixed-bed column, through which breakthrough curves, are used to analyse the performance of fixed-bed columns. The mechanisms underlying this adsorption include axial dispersion, film diffusion resistance, intraparticle diffusion resistance (both pore and surface diffusion), and sorption equilibrium with the sorbent [11,12,16]. Thomas, bed depth service time (BDST), Yoon–Nelson, and Clark are some of the mathematical models that have been used to forecast the breakthrough curve and model parameters. To create the procedure for the columns, the characteristics of parameters connected to the models were obtained by linear and nonlinear regression. All the models are equivalent in how they describe the adsorption fixed-bed columns based on error analysis and adsorption conditions [17]. Using Ni/MgO metal oxide for microwave exposure and thermal disintegration at 550°C, Ali [18] had developed an affordable adsorbent, called carbon nanotube. Using process variables like initial concentration, flow rate, and bed height, nanotube underwent column experiments for the removal of arsenite and arsenate. Thomas and Adams–Bohart models were used to examine the data, and it was discovered that the maximum removals for arsenite and arsenate, respectively, were 13.5 and 14.0 mg/g. The adsorption of cesium was studied using synthetic adsorbents, specifically polyacrylonitrile-potassium cobalt hexacyanoferrates and polyacrylonitrile-potassium nickel hexacyanoferrates. On the adsorption of cesium, the effects of liquid flow rate, bed height, and the presence of other cations were examined. The experimental data were analysed using the BDST model and the Thomas model, and the model's parameters were assessed [16,19]. Adams–Bohart, Thomas, and BDST were used by López-Cervantes et al. [20] in their investigation of fixed bed isotherm mathematical modelling. The BDST model demonstrated strong correlation coefficient values and good agreement with the experimental data. The maximum capacity for dye removal capacity was found to be 343.59 mg/g. The objective of the current study is to explore the phenol removal capability of locally available soils using a fixed-bed adsorption column study. Investigation is done into how the performance of the column is affected by bed height, concentration, and flow rate. The models Adams–Bohart, Thomas, and BDST are used to study the breakthrough curves.

2. Methodology

2.1. Preparation of adsorbents

The soil used in the study was from the Kalathur soil series at Thanjavur, Tamil Nadu, and India. Kalathur is situated in Thanjavur district, Tamil Nadu, with latitude = 10.34 and longitude = 79.20. The Kalathur soil series consists of very dark grey-brown, very deep, calcareous, fine textured Cauvery River alluvium. The soil is classified as vertisols. Vertisols are weathered soils and are poorly drained, with relatively low native fertility. Vertisols consist mainly of quartz, kaolinite, oxides, and organic matter. They appear structure less and have the feel of a loamy texture. While some are loamy or even coarser textured, many have a fine or very-fine particle-size class, but the clay is aggregated in a strong grade of fine and very fine granular structure [21].

2.2. Selection and characterization of the adsorbent

2.2.1. Soil sample

After being crushed (for 24 h in a ball mill) and sieved (with a 100–635 (0.15–0.02 mm) SIEVE NO. ASTM E11-87) to get particles with an average diameter of 0.05 mm, the soil sample was dried overnight in an electric oven at 105°C. The sample was then retrieved and conserved for later analysis by being dried, desiccated, and kept in airtight containers. To determine the soils' fundamental features, physical and chemical investigations were performed (IS: 1527 (1960)) [22]. The samples were treated with increments of 5 mL of 30% H_2O_2 in a water bath at 80°C to eliminate organic materials. The absence of effervescence suggested that all organic debris had been completely removed.

2.2.2. X-ray diffraction analysis for the soil sample

X-ray diffraction is an effective tool for qualitative mineralogical analysis. The Kr soil minerals were characterized by of X-ray diffraction peaks at diffraction angles of 21.208, 26.985 and 50.509. The major mineral components found in the two soils are quartz (Q), iron-silicon sulfide (ISS), aluminium oxide (AO), iron-silicon (IS), geothite (G), and iron oxide hydroxide (IOH). Iron oxides (like hematite and goethite) were found in the soil fractions too. The test was performed on Bruker D8 Focus under an alternating voltage of 40 kV and a current of 40 mA. Samples were subjected to CuKα radiation. The 2θ step size for the analysis ranged from 20° to 80°. The Fourier-transform infrared spectroscopy (FTIR) spectrum soil was analyzed and the percentage transmission for various wave numbers, absorption bands

identified in the spectra and their assignment to the corresponding functional group (the author published X-ray fluorescence, FTIR and scanning electron microscopy data published elsewhere).

2.2.3. Preparation of the adsorbate

The analytical reagent grade phenol (C_6H_5OH) was used to make synthetic adsorbate solutions with a range of initial concentrations (C_o) between 10 and 100 mg/L. To prepare one liter of phenol for future research, the required amount of phenol was accurately weighed and combined phase-wise with distilled water. Daily preparation and storage of the new phenol solution in a 5-L dark-colored glass container prevented photo-oxidation. Each experimental research began with a determination of the initial concentration (C_o).

2.3. Column adsorption studies

A soil adsorbent was contained in a glass column with an internal diameter of 2.50 cm and a length of 30 cm as a fixed bed adsorber. Glass wool and glass beads were used to support and seal the bed, ensuring even liquid distribution. To ensure that the particles were tightly packed and free of cavities, channels, or fissures, the bed was rinsed with distilled water and left to dry overnight. To prevent channeling of the effluent, the phenol solution was fed through a bed of soil packed adsorbent in an up-flow mode. At the entrance and outflow, a peristaltic pump was employed to regulate the flow rate. Periodically, effluent samples were taken, and their remaining phenol concentrations were measured (C_t). Therefore, 10% of the input feed concentration (100 mg/L), or 0.1 C_t/C_o or 10 mg/L, was chosen as the target breakthrough concentration (C_b). The flow through the tested column was kept going until the exhaustion point, which was indicated by the column effluent's phenol concentration approaching 0.9 C_t/C_o (C_x). The breakthrough curve is the relationship between C_t/C_o and volume treated between C_b and C_x.

Adsorption capacity calculations are made based on plots of the concentration vs. time. Curves are integrated analytically to obtain capacities measured in time units. The time required for a bed to become totally saturated is obtained by integrating as time goes to infinity [19]:

$$t_t = \int_0^\infty \left(1 - \frac{C}{C_o}\right) dt \tag{1}$$

where t_t time for total capacity, in operation, the process is to be stopped the process before solute gets breaks-through, the integration to the breakpoint time gives the "usable" capacity:

$$t_{\text{Usable}} = \int_0^{t_{\text{break}}} \left(1 - \frac{C}{C_o}\right) dt \tag{2}$$

The graph's '*S*' shape can vary significantly depending on the situation. There is usually a long period of time before the effluent concentration rises sharply and then levels off. We would expect the inlet and outlet concentrations to be the same if all of the sites were occupied. The 'breakpoint' is the point at which the fluid's outlet concentration begins to rise, and the 'exhaust point' is the point at which the effluent concentration almost equals the influent concentration. The breakthrough curve is very steep for a narrow MTZ. If the mass transfer rate is faster and there is no axial dispersion, the MTZ width is zero and the breakthrough curve is vertical. In the fixed-bed process, mass transfer resistance is critical. The overall dynamics of the system determine the system's efficiency.

Adsorption capacity calculations are made based on plots of the concentration vs. time. Curves are integrated analytically to obtain capacities measured in time units. The time required for a bed to become totally saturated is obtained by integrating as time goes to infinity:

$$t_t = \int_0^\infty \left(1 - \frac{C}{C_o}\right) dt \tag{3}$$

where t_t time for total capacity, in operation, the process is to be stopped the process before solute gets breaks-through, the integration to the breakpoint time gives the "usable" capacity:

$$t_{\text{Usable}} = \int_0^{t_{\text{break}}} \left(1 - \frac{C}{C_o}\right) dt \tag{4}$$

2.3.1. BDST model

The effects of process variables on the bed performance were studied, these included flow rate and bed depth. The three different flow rates: 10, 20 and 30 mL/min, were compared at a constant bed depth. The studied bed depths were 5, 10, and 15 cm. After the volume of breakthrough (V_b) and time of breakthrough (T_b) were determined, the BDST curves were plotted between T_b vs. bed depth (D).

According to Adams–Bohart model, the relationship between T_b and D is described as in the following equation [23].

$$T_b = \frac{N_o D}{C_o V} - \frac{1}{KC_o} \ln\left[\frac{C_o}{C_b} - 1\right] \tag{5}$$

The equation of a straight line on BDST curve is expressed as $y = ax + b$; where y = service time, x = bed depth, a = slope, and b = ordinate intercept. The numerical value of the slope $a = N_o/C_oV$ and the intercept $b = [-1/KC_o]$ $[\ln[C_o/C_b - 1]]$.

The adsorptive capacity of the system, N_o, and the rate constant, K, can be evaluated from the slope and intercept of a straight line, respectively. The minimum bed depth (D_{min}) can be calculated from the relationship of Eq. (5) by letting $T_b = 0$ and solving for D [24].

2.3.2. Empty bed contact time

Empty bed contact time (EBCT) is the time a fluid spends in the column, on the basis that the column is empty (Cooney, 1999). EBCT can be defined as follows:

$$\text{EBCT}(\text{min}) = \frac{\text{Bed Volume in cm}^3}{\text{Volume flowrate in cm}^3/\text{min}} \quad (6)$$

2.3.3. Adams–Bohart column model

Adams–Bohart established the fundamental relationship between C/C_o and t for the adsorption of chlorine on charcoal in 1920. However, this model was equally good for other systems also and therefore adopted by several researchers. Adams–Bohart A model was used to describe the initial part of the breakthrough curve.

$$\ln\left(\frac{C_t}{C_0}\right) = K_{AB}C_0 - \frac{K_{AB}N_0Z}{F} \quad (7)$$

where C_o — initial concentration of phenol, C_t — concentration of effluent at time, F —linear velocity calculated by dividing the flow rate by the column section area (cm/min), K_{AB} – Adams–Bohart rate constant (L/mg·min), N_o — adsorption capacity of the adsorbent (mg/L) and Z — bed depth of the column (cm). A plot is plotted between $\ln(C_t/C_o)$ vs. t.

3. Results and discussion

3.1. Design of a column studies

In the present study analysis of fixed column adsorption studies of phenol onto the soils were investigated. Adams–Bohart, BDST, and EBCT are a few of the mathematical models used to forecast the breakthrough curve and model parameters. To create the procedure for the columns, linear regression was used to acquire the properties of the model-related parameters. The results showed that a decrease in flow rate at a constant bed depth increased the breakthrough volume (V_b) and therefore the breakthrough time (T_b), due to an increase in EBCT. At the flow rate of 10 mL/min and at varying depths 5, 10 and 15 cm the EBCT was found 2.45, 4.91 and 7.36 min. The adsorption capacity (N_o) of soil was calculated to be 713.37, 978.34 and 978.34 mg/L by using the flow rates of 10, 20 and 30 mL/min. The results of the examination of the dynamic adsorption system were also demonstrated to be significantly influenced by the modelling methodology.

Fig. 1 shows the effect of flow rates namely 10, 20 and 30 mL/min on the soil adsorbent (Kr soil) breakthrough curves by using a bed depth of 5 cm. When the adsorption zone moves up and the upper edge of this zone reaches the top of the column, the effluent concentration starts to rise rapidly [23,25]. This point is called the breakthrough point, corresponding volume of effluent collected indicated as V_b. The results showed that a decrease in flow rate at a constant bed depth increased the V_b and therefore the T_b, due to an increase in EBCT. Since the front of adsorption zone reached the top of the column later by using a slower flow rate, more V_b was obtained. The results show that the breakthrough curve was obtained quickly with higher flow rates. The time required to reach saturation increased significantly with a decrease in flow rate. The column was run with flow rates of 10, 20 and 30 mL/min and bed depth of the column 10 cm as shown in Fig. 2. The results show that the breakthrough curve was obtained quickly with higher flow rates but compared with Fig. 1 the time required to reach saturation increased significantly with an increase in the bed depth. Further increase in bed depth from 10 to 15 cm and the effect of flow rates were studied. The time required to reach saturation increased significantly with a decrease in flow rate (Fig. 3).

The breakthrough curve of the lower flow rate (10 mL/min) (Fig. 4) shows steep rise near the exhaustion point, suggesting that the adsorption zone was shorter, and the adsorbent was more completely saturated with the phenol [26,27]. Fig. 5 represents the breakthrough curve at a flow

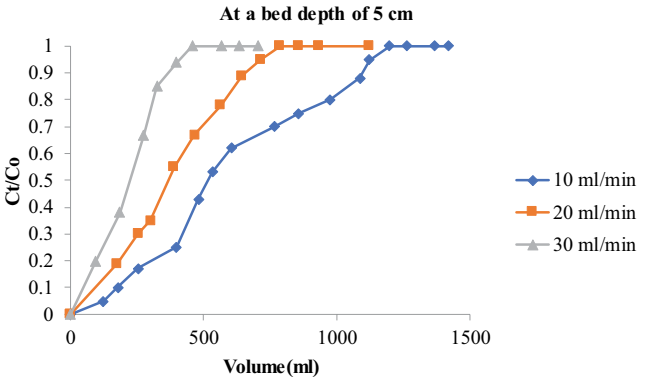

Fig. 1. Effect of flow rate on 5 cm depth.

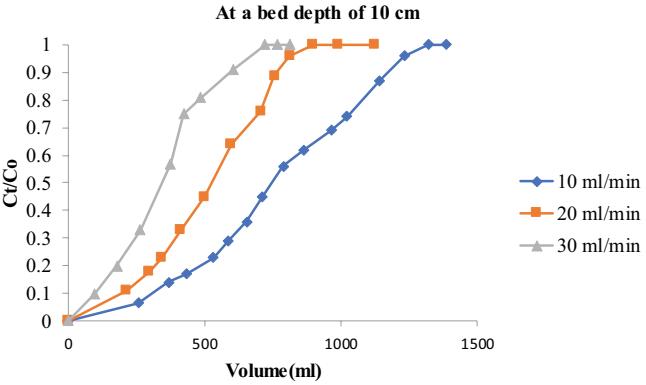

Fig. 2. Effect of flow rate on 10 cm depth.

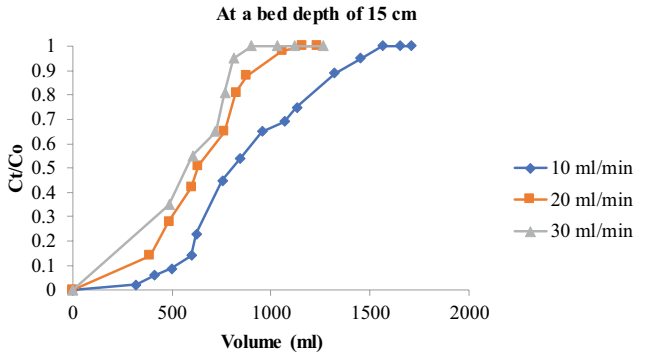

Fig. 3. Effect of flow rate on 15 cm depth.

rate of 20 mL/min and are very steep compared to the breakthrough curves at a flow rate of 10 mL/min. This is because the flow rate is large and the contact time is very short. The zone of adsorption was very shallow. Fig. 6 also shows that the breakthrough curve of 30 mL/min became less sharp because the adsorption zone was deeper. This result suggests that a lower flow rate or a longer contact time may be required for phenol adsorption by a column of soil adsorbent and the results comply with the results of other researchers [28]. Table 1 shows the details of bed depth (i.e., 5, 10 and 15 cm) and flow rate (i.e., 10, 20 and 30 mL/min), the column studies were conducted by varying flow rate and varying the depth of the column bed. At the flow rate of 10 mL/min and at varying depths 5, 10 and 15 cm the EBCT was found 2.45, 4.91 and 7.36 min. Similarly for a flow rate of 20 and 30 mL/min, at varying depths 5, 10 and 15 cm, the EBCT was found 1.23, 2.45 and 3.68 min and 0.82, 1.64 and 2.45 min, respectively. For these test columns, the optimum flow rate should not be higher than 10 mL/min to provide a shorter adsorption zone and a longer service time. The researchers studied EBCTs at different flow rates for the adsorption of AB1 and AB113. The present findings agree with the results reported by the Samarghandi et al. [29].

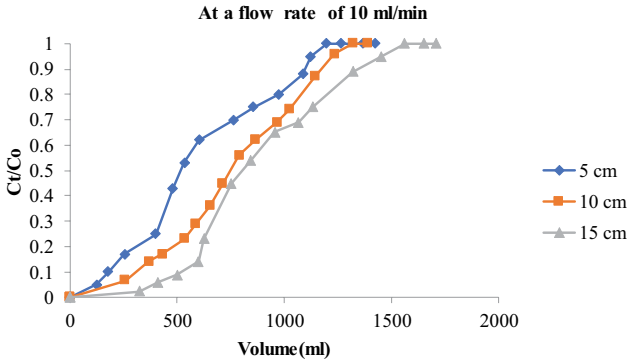

Fig. 4. Effect of bed depth for a flow rate of 10 mL/min.

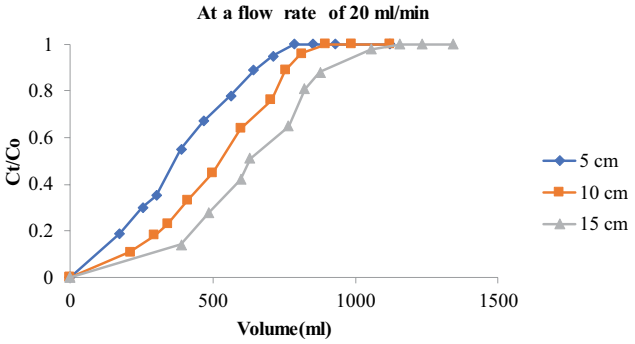

Fig. 5. Effect of bed depth for a flow rate of 20 mL/min.

3.2. Effect of bed depth on breakthrough curve

Figs. 4–6 show the breakthrough curves of different bed depths at constant flow rates of 10, 20 and 30 mL/min, respectively. V_b or T_b increased with increasing bed depth while the shape and gradient of the breakthrough curves were slightly different with the variable bed depths. However, the breakthrough curves of the longer beds tended to be more gradual. This may be because of the reason that the column was difficult to be completely exhausted. This effect was higher by using the higher flow rate of 30 mL/min (Fig. 6). This study indicated that the flow rate at the outlet was unstable when the bed depth was too high due to a higher flow resistance, which resulted from a tighter packing of the longer bed containing more amount of adsorbent. Although an increasing bed depth increased V_b or T_b, too high bed depth is not useful for a single column; otherwise, the multiple beds need to be designed. Since the treated effluent was not properly drawn off at the top of the packed bed higher than 15 cm for the diameter

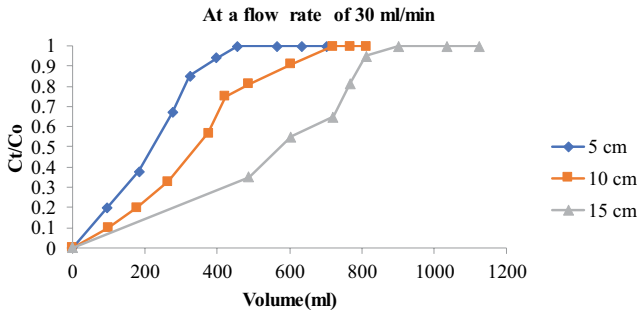

Fig. 6. Effect of bed depth for a flow rate of 30 mL/min.

Table 1
Details of bed depth and flow rate in fixed bed column

Q (mL/min)	Bed depth (cm)	Bed volume (cm^3)	W_c (g)	EBCT (min)	V_b (mL)	T_b (min)	Usage (g/mL)
	5	24.5313	5.13	2.45313	95	16	0.054
10	10	49.0625	10.26	4.90625	225	28	0.0456
	15	73.5938	15.39	7.35938	356	56	0.04323
	5	24.5313	5.13	1.22656	67	5	0.07657
20	10	49.0625	10.26	2.45313	167	15	0.06144
	15	73.5938	15.39	3.67969	254	31	0.06059
	5	24.5313	5.13	0.81771	43	2	0.1193
30	10	49.0625	10.26	1.63542	100	8	0.1026
	15	73.5938	15.39	2.45313	156	15	0.09865

of 2.5 cm, the optimum depth-to-diameter ratio of column containing agro-based adsorbent should be lower than or equal to 6 (15/2.5). Actually, this ratio can be applied for the scale up of the column adsorber.

3.3. BDST with variation in bed depth and flow rate

The data of EBCT, V_b and T_b increased with decreasing flow rate or increasing bed depth. However, the flow rate should not be too low, depending on the detention time and the volume of wastewater for treatment. As mentioned above, the bed depth should also not be too high; therefore, the multiple beds operated in series or parallel should be preferable. From the data in Tables 1 and 2, the BDST plots (T_b vs. D) were constructed, as shown in Figs. 7 and 8. The equations of linear relationship were obtained with all R^2 above 0.96. The minimum bed depth (D_{min}), the adsorption capacity (N_o) and the rate constant (K) were calculated, as shown in Table 2. The results showed that D_{min} was higher when the flow rate was increased because the adsorption zone must be increased to remove the phenol under the higher flow rate. In the column diameter of 2.5 cm, the actual bed depth of soil for the flow rate of 10, 20 and 30 mL/min should be greater than 0.67, 1.53 and 2.50 cm, respectively, which means a sufficient length of adsorption zone was necessary to attain a satisfactory effluent or to prevent the effluent solute concentration from exceeding 10 mg/L at zero time under test conditions. The adsorption capacity (N_o) of soil was calculated to be 713.37, 978.34 and 978.34 mg/L by using the flow rates of 10, 20 and 30 mL/min. However, N_o and k did not show consistent trend for initial flow rates and concentration. The similar trend was observed by Daffalla et al. [30], it was found that the capacity of bed adsorption increased according to the increase in the influent concentration and bed depth. However, the capacity of bed adsorption decreased according to the increase in the feed flow rate. These findings agree with the results reported by Sarkar and Das [31] and Madan et al. [32] in similar studies.

3.4. Adams–Bohart column modelling

As mentioned earlier Adams–Bohart model is used for the prediction of initial part of the breakthrough curves. The model parameters are given in Table 3. The table exhibits the effect of bed height and flow velocity. It could be seen from Figs. 9–11 that Adams–Bohart plot exhibits multi-linearity. Thus, it is possible to predict the breakthrough curve using Adams–Bohart model parameters evaluated at different service times.

The values of maximum adsorption capacity (N_o) and Adams–Bohart rate constant (K_{AB}) were determined from the intercept and slope of Adams–Bohart plot at different bed height and flow rates as shown in Table 3. The maximum adsorption capacity (N_o) value increased when the flow rate increased (Table 3), but it did the opposite as the bed height increased. It has the best fits out of all the models, with R^2 values in the 0.92–0.99 region, showing that the model has strong applicability. The values of K_{AB} were found to decrease with increase in flow rate and while its value increased with increase in bed height (Table 3) indicating that the overall system kinetics was dominated by external mass transfer while its value increased with increase in bed height (Table 3). Of all the models, has the best fittings with R^2 values in the range 0.92–0.99 indicating that the model has good applicability. The present findings agree with the results reported by Samarghandi et al. [29].

3.5. Dynamic column studies

A glass column of 30 cm length and 2.50 cm diameter was used to contain soil and soil-agro blend adsorbent as a fixed-bed adsorber. The experiments were carried out on different flow rates for different depths. The theoretical adsorption capacity of an adsorbent at any final concentration can be calculated by making use of any one best

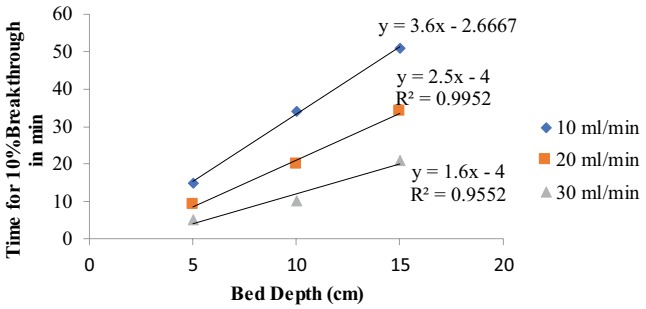

Fig. 7. Bed depth service time curves for 10% breakthrough.

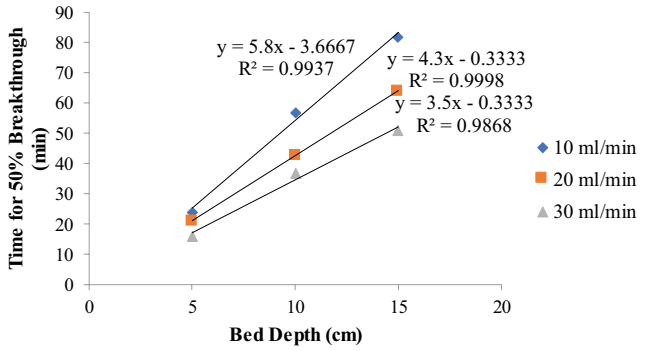

Fig. 8. Bed depth service time curves for 50% breakthrough.

Table 2
Constants of BDST equations

Q (mL/min)	V (cm/min)	Slope	Intercept	D_{min} (cm)	N_o (mg/L)	K (L/mg·min)
10	2.038217	26.1	–35.66	1.366284	53.19745	0.000616
20	4.076433	18.3	–21.66	1.183607	74.59873	0.001014
30	6.11465	11.6	–17.33	1.493966	70.92994	0.001268

Table 3
Adams–Bohart model parameters

Sl. No.	Flow rate (mL/min)	C_o (mg/L)	Bed height (cm)	K_{AB}	N_o (mg/L)	R^2
			5	0.014513	728.70	0.92
1	10	100	10	0.016305	457.08	0.96
			15	0.025844	318.32	0.94
			5	0.011142	1,257.51	0.95
2	20	100	10	0.01798	810.86	0.99
			15	0.019384	599.39	0.93
			5	0.01227	1,712.86	0.93
3	30	100	10	0.010067	2,172.33	0.97
			15	0.015269	1,141.40	0.93

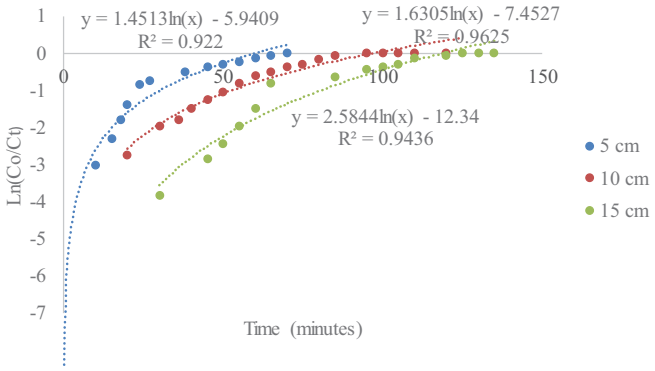

Fig. 9. Adams–Bohart model (C_o 100 ppm, flow rate 10 mL/min).

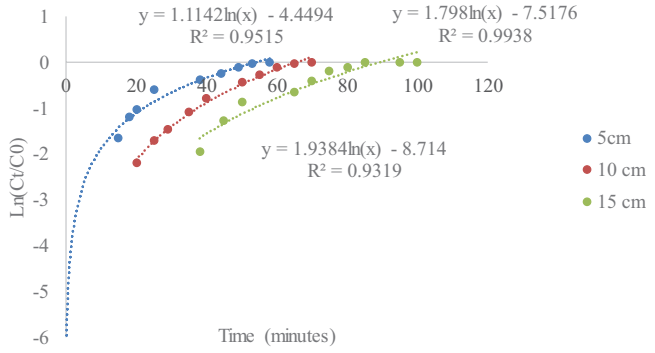

Fig. 10. Adams–Bohart model (C_o 100 ppm, flow rate 20 mL/min).

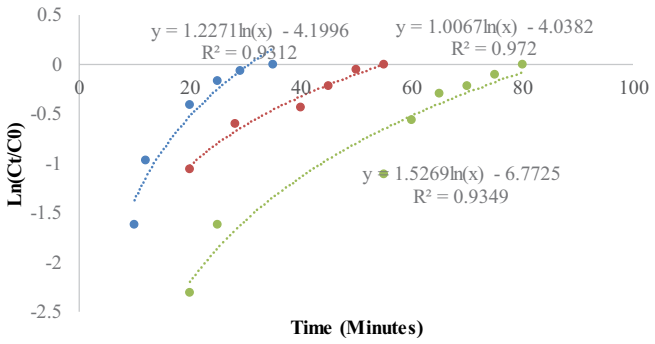

Fig. 11. Adams–Bohart model (C_o 100 ppm, flow rate 30 mL/min).

isotherm model. The value of the adsorptive capacity thus obtained represents the amount of adsorbate adsorbed per unit weight of the adsorbent when effluent the effluent concentration equals to the for estimation by making use of the breakthrough curve. Breakthrough being defined as the point when a specified amount of the influent is detected in the effluent [33]. A breakthrough of 10% occurs when the concentration of the effluent is 10% of the influent concentration [34–36]. Influent phenol concentration of about 100 mg/L was used for all the attempted influent concentration and 90% breakthrough occurs when the concentration of the effluent is 90% of the influent concentration. The area between the ordinate and the breakthrough curve gives the concentration of the adsorbate removed over the test time. The amount of adsorbate removed per gram of adsorbent is then obtained by dividing the total amount of adsorbate removed by the mass of the adsorbent in the column. A continuous flow study was performed to compare the adsorption capacity obtained from a continuous column experiment to those determined from batch studies.

3.6. X-ray diffraction analysis for the soil sample

X-ray diffraction is an effective tool for qualitative mineralogical analysis. The soil minerals were characterized by X-ray diffraction peaks at diffraction angles of 21.208, 26.985 and 50.509. Hematite, a common iron oxide with the chemical formula Fe_2O_3, has a distinctive peak in the 2θ scale between 33 and 36 and is what gives soil its red colour. While being the most prevalent of iron oxides, goethite (which has a molecular structure of FeOOH) exhibits a distinctive peak between 20 and 22 and is what gives soil its yellow colour. The soil samples contained these minerals. Gibbsite was another mineral, and its primary peak was at roughly 25.0° 2θ. Quartz was also observed in the X-ray diffraction analysis. This mineral exhibits characteristics peaks around 22 and 27.0 in the 2θ scale.

4. Conclusions

In a column investigation, soil (Kalthur soil) was found to be capable of dephenolation from aqueous phenolated solution to a degree comparable to commercial activated carbon, but at a significantly lower cost. The design parameters bed depth and flow rate for an adsorption bed were

determined based on column studies. The optimal rate of flow of 10 mL/min, the D_{min} was determined to be 4 cm for a bed depth of up to 14 cm. According to the Adams–Bohart model, K_{AB} values were observed to rise with rising flow rates while falling with rising bed heights. Although the maximum adsorption capacity (N_o) value decreased with an increase in bed height, it increased with an increase in flow rate. Regarding the analysis of soil sample the FTIR record shows that these samples include a wide range of functional groups, such as lactones, phenols, ethers, and carboxyl. The adsorbent's FTIR analysis before and after adsorption revealed distinct spectrum changes, including band disappearance and spectral shifts and expansions. Adsorption alters the peaks of –C–O–C bonds, the –C=C, C–O, and aliphatic (–CH_3 and –CH_2) functional groups, as well as adsorbent-specific oscillations in the –OH group, among other things.

References

[1] A. Panagopoulos, V. Giannika, Comparative techno-economic and environmental analysis of minimal liquid discharge (MLD) and zero liquid discharge (ZLD) desalination systems for seawater brine treatment and valorization, Sustainable Energy Technol. Assess., 53 (2022) 102477, doi: 10.1016/j.seta.2022.102477.

[2] A. Panagopoulos, Brine management (saline water & wastewater effluents): sustainable utilization and resource recovery strategy through minimal and zero liquid discharge (MLD & ZLD) desalination systems, Chem. Eng. Process. Process Intensif., 176 (2022) 108944, doi: 10.1016/j.cep.2022.108944.

[3] A. Panagopoulos, Techno-economic assessment and feasibility study of a zero liquid discharge (ZLD) desalination hybrid system in the Eastern Mediterranean, Chem. Eng. Process. Process Intensif., 178 (2022) 109029, doi: 10.1016/j.cep.2022.109029.

[4] S.M. Ho, Low-cost adsorbents for the removal of phenol/phenolics, pesticides, and dyes from wastewater systems: a review, Water, 14 (2022) 3203, doi: 10.3390/w14203203.

[5] M.N. Abbas, A.-S.T. Al-Madhhachi, S.A. Esmael, Quantifying soil erodibility parameters due to wastewater chemicals, Int. J. Hydrol. Sci. Technol., 9 (2019) 550–568.

[6] H.T. Hamad, Removal of phenol and inorganic metals from wastewater using activated ceramic, J. King Saud Univ. Eng. Sci., 33 (2021) 221–226.

[7] V.K. Gupta, I. Ali, T.A. Saleh, M.N. Siddiqui, S. Agarwal, Chromium removal from water by activated carbon developed from waste rubber tires, Environ. Sci. Pollut. Res., 20 (2013) 1261–1268.

[8] S.M. Anisuzzaman, A. Bono, D. Krishnaiah, Y.Z. Tan, A study on dynamic simulation of phenol adsorption in activated carbon packed bed column, J. King Saud Univ. Eng. Sci., 28 (2016) 47–55.

[9] M. Malakootian, H.J. Mansoorian, M. Alizadeh, A. Baghbanian, Phenol removal from aqueous solution by adsorption process: study of the nanoparticles performance prepared from *Aloe vera* and *Mesquite* (Prosopis) leaves, Sci. Iran. C, 24 (2017) 3041–3052.

[10] M.F. Abid, O.N. Abdulla, A.F. Kadhim, Study on removal of phenol from synthetic wastewater using solar photocatalytic reactor, J. King Saud Univ. Eng. Sci., 31 (2019) 131–139.

[11] F. Kafshgari, A.R. Keshtkar, M.A. Mousavian, Study of Mo(VI) removal from aqueous solution: application of different mathematical models to continuous biosorption data, Iran. J. Environ. Health Sci. Eng., 10 (2013) 14, doi: 10.1186/1735-2746-10-14.

[12] N. Miralles, C. Valderrama, I. Casas, M. Martínez, A. Florido, Cadmium and lead removal from aqueous solution by grape stalk wastes: modeling of a fixed-bed column, J. Chem. Eng. Data, 55 (2010) 3548–3554.

[13] G. Vázquez, R. Alonso, S. Freire, J. González-Álvarez, G. Antorrena, Uptake of phenol from aqueous solutions by adsorption in a *Pinus pinaster* bark packed bed, J. Hazard. Mater., 133 (2006) 61–67.

[14] L.F. Bautista, M. Martínez, J. Aracil, Adsorption of α-amylase in a fixed bed: operating efficiency and kinetic modeling, AlChE J., 49 (2003) 2631–2641.

[15] C.-C. Chen, K.F. Hayes, X-ray absorption spectroscopy investigation of aqueous Co(II) and Sr(II) sorption at clay–water interfaces, Geochim. Cosmochim. Acta, 63 (1999) 3205–3215.

[16] H. Patel, Fixed-bed column adsorption study: a comprehensive review, Appl. Water Sci., 9 (2019) 45, doi: 10.1007/s13201-019-0927-7.

[17] L. Rafati, M.H. Ehrampoush, A.A. Rafati, M. Mokhtari, A.H. Mahvi, Fixed bed adsorption column studies and models for removal of ibuprofen from aqueous solution by strong adsorbent nano-clay composite, J. Environ. Health Sci. Eng., 17 (2019) 753–765.

[18] I. Ali, Microwave assisted economic synthesis of multi walled carbon nanotubes for arsenic species removal in water: batch and column operations, J. Mol. Liq., 271 (2018) 677–685.

[19] L. Hao, Q. Liu, X. Li, Z. Du, P. Wang, A potentially low-cost modified sawdust (MSD) effective for rapid Cr(VI) and As(V) removal from water, RSC Adv., 91 (2014) 49569–49576.

[20] J. López-Cervantes, D.I. Sánchez-Machado, R.G. Sánchez-Duarte, M.A. Correa-Murrieta, Study of a fixed-bed column in the adsorption of an azo dye from an aqueous medium using a chitosan–glutaraldehyde biosorbent, Adsorpt. Sci. Technol., 36 (2018) 215–232.

[21] S.V.G. Rajan, H.G.G. Rao, Studies of Soils of India, Vikas Publishing House Pvt., Ltd., New Delhi, 1987.

[22] Indian Standard Methods of Chemical Analysis of Fireclay and Refractory Materials, IS: 1527, 1960.

[23] S.D. Faust, O.M. Aly, Adsorption Process for Water Treatment, Butterworths Publishers, Stoneham, 1987.

[24] B. Volesky, I. Prasetyo, Cadmium removal in a biosorption column, Biotechnol. Bioeng., 43 (1994) 1010–1015.

[25] T. Mpouras, A. Polydera, D. Dermatas, N. Verdone, G. Vilardi, Multi wall carbon nanotubes application for treatment of Cr(VI)-contaminated groundwater; modeling of batch & column experiments, Chemosphere, 269 (2021) 128749, doi: 10.1016/j.chemosphere.2020.128749.

[26] J. Zhao, L. Yu, H. Ma, F. Zhou, K. Yang, G. Wu, Corn stalk-based activated carbon synthesized by a novel activation method for high-performance adsorption of hexavalent chromium in aqueous solutions, J. Colloid Interface Sci., 578 (2020) 650–659.

[27] A. Mandal, S.K. Das, Adsorptive removal of phenol by activated alumina and activated carbon from coconut coir and rice husk ash, Water Conserv. Sci. Eng., 4 (2019) 149–161.

[28] J. Cruz-Olivares, C. Pérez-Alonso, C. Barrera-Díaz, F. Ureña-Nuñez, M.C. Chaparro-Mercado, B. Bilyeu, Modeling of lead(II) biosorption by residue of allspice in a fixed-bed column, Chem. Eng. J., 228 (2013) 21–27.

[29] M.R. Samarghandi, M. Hadi, G. McKay, Breakthrough curve analysis for fixed-bed adsorption of azo dyes using novel pine cone—derived active carbon, Adsorpt. Sci. Technol., 32 (2014) 791–806.

[30] S.B. Daffalla, H. Mukhtar, M.S. Shaharun, A.A. Hassaballa, Fixed-bed adsorption of phenol onto microporous activated carbon set from rice husk using chemical activation, Appl. Sci., 12 (2022) 4354, doi: 10.3390/app12094354.

[31] S. Sarkar, S.K. Das, Removal of hexavalent chromium from aqueous solution using natural adsorbents - column studies, Int. J. Eng. Res. Technol. (IJERT), 5 (2016) 370–377.

[32] S.S. Madan, B.S. De, K.L. Wasewar, Adsorption performance of packed bed column for benzylformic acid removal using CaO_2 nanoparticles, Chem. Data Collect., 23 (2019) 100267, doi: 10.1016/j.cdc.2019.100267.

[33] M. LaGrega, P. Buckingham, J. Evans, The Environmental Resources Management Group, Hazardous Waste Management, McGraw-Hill Inc., New York, NY, 1994.

[34] R.A. Dobbs, J.M. Carbon, Adsorption Isotherms for Toxic Organics, Municipal Environmental Research Laboratory, Office of Research and Development, USEPA, Cincinnati, Ohio, 1980.
[35] Metcalf and Eddy, Wastewater Engineering Treatment and Reuse, TATA McGraw-Hill, 2005.
[36] W.J. Wujcik, W.L. Lowe, P.J. Marks, W.E. Sisk, Granular activated carbon pilot treatment studies for explosives removal from contaminated groundwater, Environ. Prog., 11 (1992) 178–189.